Received: 2 September 2019 | Revised: 24 February 2020 | Accepted: 25 February 2020

DOI: 10.1111/pce.13750

TECHNICAL REPORT

Plant, Cell & Environment WILEY

The DroughtBox: A new tool for phenotyping residual branch conductance and its temperature dependence during drought

Lise M. Billon† | Chris J. Blackman† | Hervé Cochard | Eric Badel | Adnane Hitmi | Julien Cartailler | Romain Souchal | José M. Torres-Ruiz

Université Clermont-Auvergne, INRAE, PIAF, Clermont-Ferrand, France

Correspondence
José M. Torres-Ruiz, Université Clermont-Auvergne, INRAE, PIAF, 63000 Clermont-Ferrand, France.
Email: torresruizjm@gmail.com

Funding information
Agence Nationale de la Recherche, Grant/Award Number: ANR-18-CE20-0005 Hydrauleaks

Abstract

Xylem hydraulic failure is a major driver of tree death during drought. However, to better understand mortality risk in trees, especially during hot-drought events, more information is required on both rates of residual water-loss from small branches (g_{res}) after stomatal closure, as well as the phase transition temperature (T_p), beyond which g_{res} significantly increases. Here, we describe and test a novel low-cost tool, the DroughtBox, for phenotyping g_{res} and T_p across species. The system consists of a programmable climatically controlled chamber in which branches dehydrate and changes in the mass recorded. Test measurements show that the DroughtBox maintains stable temperature and relative humidity across a range of set points, a prerequisite for getting accurate g_{res} and T_p values. Among a study group of four conifer and one angiosperm species, we observed a range of g_{res} (0.44–1.64 mmol H_2O m^{-2} s^{-1}) and T_p (39.4–43.8°C) values. Furthermore, the measured time to hydraulic failure varied between two conifers species and was shortened in both species following a heatwave event. The DroughtBox is a reliable and customizable tool for phenotyping g_{res} and T_p, as well as for testing models of time to hydraulic failure that will improve our ability to assess climate change impacts on plants.

KEYWORDS

drought, DroughtBox, heatwave, leaf cuticle, minimum conductance (g_{min}), phase transition temperature (T_p), residual conductance (g_{res})

1 | INTRODUCTION

Global warming is triggering massive tree mortality events worldwide due to an increase in the frequency of heat waves and extreme drought events (Allen et al., 2010; Choat et al., 2012). As soil dries out under drought conditions, increasing tension within the water conducting xylem can exceed a threshold value causing cavitation and the formation of air-embolisms that block water flow, causing catastrophic hydraulic failure and leading to plant death (Tyree, 1989). Plants may reduce the risk of hydraulic failure during drought by evolving xylem tissue that is highly resistant to cavitation and/or by maintaining favourable plant water status through stomatal closure and low residual transpiration (Sperry, Alder, & Eastlack, 1993). Characterizing how different plant species modulate these traits will determine their risk of drought-induced mortality (Choat et al., 2012) and is crucial for predicting how climate change will affect species distribution and vegetation composition worldwide (Jentsch, Kreyling, & Beierkuhnlein, 2007).

Cavitation resistance is one of the most studied traits involved in tree mortality and it is evaluated by determining P_{50} which corresponds to the xylem pressure inducing 50% of loss of conductance (Tyree & Ewers, 1991). Cavitation resistance is correlated with environmental

†Equal contributors.

conditions related to water availability, with more vulnerable trees (i.e., higher P_{50} values) generally growing in high rainfall environments (Blackman, Brodribb, & Jordan, 2012; Brodribb & Hill, 1999; Choat et al., 2012). However, P_{50} may not be sufficient alone for assessing species drought-response strategy and explaining differences in their spatial distribution. For example, relatively high P_{50} values of between −1 to −2 MPa have been reported for baobab trees occurring in extremely dry and hot deserts (Chapotin, Razanameharizaka, & Holbrook, 2006). Therefore, in addition to P_{50}, it is important to evaluate other traits related species drought response strategy, such as hydraulic capacitance (Gleason, Blackman, Cook, Laws, & Westoby, 2014), stomatal closure (Arve, Torres, Olsen, & Tanino, 2011; Blackman et al., 2019; Creek et al., 2020) and residual conductance (Burghardt & Riederer, 2003; Martin-StPaul, Delzon, & Cochard, 2017).

Stomatal functioning and behaviour have been studied for decades (Darwing 1898). In most species under non-limiting water conditions, stomata open during the day to acquire atmospheric CO_2 for photosynthesis while at the same time lose water due to transpiration. To avoid desiccation during drought, plants close their stomata, which reduces the rate of water loss. However, even when stomata are closed, plants continue to lose water though leaf cuticles, leaky stomata and bark (lenticular conductance). These residual water losses influence the kinetics of cavitation as a consequence of their role in determining the time at which point plant water potentials reach the threshold values of hydraulic failure (Blackman et al., 2016, 2019; Martin-StPaul et al., 2017). Indeed, simulations with a recently developed mechanistic model ('SurEau' model, Martin-StPaul et al., 2017) show how residual conductance is a principal determinant of the onset of hydraulic failure.

Following stomatal closure, residual leaf transpiration mainly occurs through the cuticle, but can also occur to a largely unknown extent through leaky stomata. These residual water losses are collectively termed as the leaf minimum conductance, or g_{min} (Schuster, Burghardt, & Riederer, 2017), and is determined by its conductance to water vapor and the vapor pressure deficit (VPD) between the leaf and the air. Observations to date suggest that g_{min} varies across species (Duursma et al., 2019; Schuster et al., 2017), although can only be correlated with environmental conditions such as rainfall in some groups of plants (Brodribb, McAdam, Jordan, & Martins, 2014). Research also suggests that g_{min} may be sensitive to increasing temperature. For example, Bueno et al. (2019) showed how g_{min} increases significantly when temperatures increase above 37.7°C for *Citrullus colocynthis*. This threshold point where g_{min} markedly increases has been called as the phase-transition temperature (T_p) and corresponds to the temperature above which cuticular permeability increases as a result of changes in the structure of cuticular waxes (Burghardt & Riederer, 2006). The T_p value is important because it gives information about the ability of plants to resist uncontrolled and rapid dehydration leading to run-away embolism during periods of high temperature (Cochard, 2019).

To date, the most widely used methodology for determining g_{min} consists of repeated measurements of detached leaves dehydrating on a bench (Burghardt & Riederer, 2003). This method, however, depends on the climatic conditions inside the lab, which if not constant will induce significant differences in water loss rate through time. This approach also makes it difficult to assess the temperature response of g_{min} and subsequent determination of T_p due to the difficulties of reaching and maintaining relatively high air temperatures. Another way to measure g_{min} under variable conditions is to place detached leaves in an incubator and control relative humidity with the addition of Silica gel (Schuster et al., 2016). Although this method can be used to determine both g_{min} and T_p, it still relies on repeated manual measurements of leaf mass.

Measurements of residual water losses from plants have mainly focused on leaf cuticles ($g_{cuticle}$) and detached leaves (g_{min}). Nevertheless, water loss from plant shoots during drought also occurs through the bark (g_{bark}), the contribution of which remains largely unknown. Thus, we define a term for the collective branch residual conductance (that is, $g_{min} + g_{bark}$) as g_{res}. Here we introduce and test a new automated tool, the DroughtBox, for phenotyping g_{res} and its possible temperature dependence T_p. The main aims of this study are i) to describe the principle and setup of the DroughtBox; ii) to demonstrate its capability to accurately regulate temperature (T) and relative humidity (RH) through time; iii) to measure g_{res} and T_p in branches from a group of four conifer and one angiosperm species; and iv) to determine the time required to dehydrate to critical levels of hydraulic failure under constant and constant × heatwave conditions.

2 | MATERIAL AND METHOD

2.1 | Description of the DroughtBox

The DroughtBox consists of a 70 cm cubic box made of 40 mm thick polystyrene boards with a front door and two compartments (Figure 1). In the upper compartment (comp. A), eight 500 g strain gauges AS05 (Wimesure, France) are fixed in an aluminium frame and connected to an acquisition board (PhidgetBridge 4-Input 1,046, Phidgets inc., Unit 1–6,115, 4 St SE, Calgary AB T2H 2H9, Canada). Branches for g_{res} measurements are placed in the main lower compartment (comp. B) and attached to the strain gauges through holes in the roof board. An air temperature and relative humidity sensor (HyT271, Innovative Sensor Technology IST AG, Switzerland) is suspended in the branch compartment to monitor changes in these two variables within the compartment. Heating resistors (HK-5,0–12 75 W, A. Rak Wärmetechnik GmbH, Germany) and heat dissipators are also placed in this compartment to enable temperature increase up to a maximum of 55°C. Relative humidity in the compartment B is adjusted by differentially injecting water-saturated or dry air with two electronically controlled valves. Both the heating resistors and the three-way valves are piloted by an Arduino MEGA 2560 to control T, RH and, therefore, VPD. Small fans, installed in the compartment B, stir the air in order to reduce spatial heterogeneities in T and RH. To induce stomatal opening in fresh, well-hydrated branches, four LED lights XLamp CXA3070 (8,646 lm and 4,000 K, CREE, North Carolina, USA) illuminate inside the box. The DroughtBox is controlled by a nano-computer Raspberry-Pi 3 (Raspberry pi Foundation, United Kingdom) that allows users to program and set up target temperatures

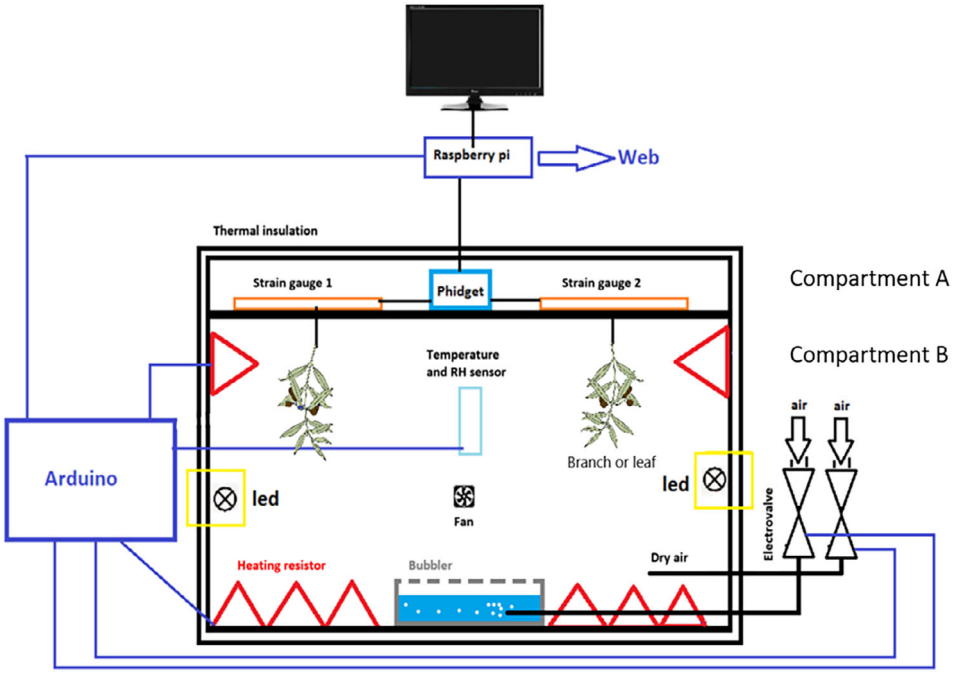

FIGURE 1 Schematic of the DroughtBox. Branches in the lower compartment are attached to strain gauges in the upper compartment, which are linked to an acquisition board PhidgetBridge and to a Raspberry Pi computer. Following hydration overnight, branches are allowed to dehydrate inside the insulated box in which temperature is controlled via heating resistors and relative humidity is controlled via the injection of either dry or humidified air. Each environmental parameter is controlled by a microcontroller, Arduino, which responds to experimenter commands. Small (4 cm diameter) fans circulates the air at a constant rate

and relative humidity conditions in the compartment B. Two programs record both the mass of the branches and the T and RH conditions at specified time steps, either under fixed or variable climate conditions.

2.2 | Plant material and sample installation

Four conifer (*Abies alba* Mill., *Picea abies* L., *Pseudotsuga menziesii* (Mirb.) *Cedrus atlantica var. glauca* (Endl.) Carri) and one angiosperm (*Quercus ilex* L.) species were used in the current study. Three of the conifers (*A. alba*, *P. abies* and *P. menziesii*) were collected at the Royat Arboretum (Royat, France, 45°45′22.8″N 3°01′26.1″E), while *C. atlantica* and *Q. ilex* were collected at INRAE of Crouël (Clermont-Ferrand, France, 45°46′30.8″N 3°08′38.2″E). Branches of 1–1.5 m in length were collected at 2–3 m height from the outer part of the crown of 6–8 trees and transported to the lab in large plastic bags. The cut end of each branch was recut and kept in water overnight while the terminal of the branches were enclosed in plastic bags and stored in dark conditions to allow full rehydration. Before their installation in the DroughtBox, each branch was recut ca. 40 cm from the tip, the cut end was sealed with paraffine wax (melting point 68°C, Fluka) and the fresh weight of the branch was immediately measured. Branches were then attached to each of eight strain gauge hooks using copper wire, after which the box was closed and the branches were allowed to dehydrate progressively.

2.3 | Performance of the DroughtBox in regulating T and RH

The capacity of the system for reaching and maintaining constant conditions of T and RH was evaluated. We set a temperature of 30°C and relative humidity of 40% for 90 consecutive hours and monitored T, RH and VPD every 5 s. We then evaluated the capacity of the system to increase T from 30 to 50°C for over a period of 20 hours with step-wise increase in T of 5°C and RH both held constant at 40% and allowed to decrease so that air-water concentration was maintained at 10.6 g.kg^{-1}.

2.4 | Determination of g_{res}

Eight branches from each of the five species were installed in the Drought-Box to determine g_{res} under fixed conditions, with T and RH set at 30°C and 40%, respectively. These values are typical of summer midday conditions in the area where the samples were collected (Clermont-Ferrand, Figure S1).

The weight w (g) of each branch was recorded at 5 min intervals. We assumed that changes in w represented water molecules (n_w, mmol) leaving the branches by transpiration which enables the calculation of E (mmol s^{-1} m^{-2}) following Equation (1):

$$E = -\frac{slope\,(n_w;t)}{LA + BA}$$

With t the time in seconds, LA the two-sided leaf area (m^2) derived from the leaf dry mass of each measured branches and empirical relationships between leaf dry mass and fresh leaf area (i.e., SLA), and BA the surface area (m^2) of the stem determined from measurements of stem length and basal diameter and assuming the shape of a cone. Finally, the g_{res} is calculated from the linear portion of the water loss curve, that is, after stomatal closure, following Equation (2):

$$g_{res} = \frac{E}{VPD} x\,101.6$$

With E the transpiration in mmol m^{-2} s^{-1}, the air VPD in kPa and 101.6 the atmospheric pressure in the DroughtBox in kPa. For calculating g_{res}, we used the driving force derived, that is, VPD, from leaf temperature measurements recorded for each species (more details below). At the end of the experiment, leaves were removed and oven-dried for 60 h for determination of leaf dry mass.

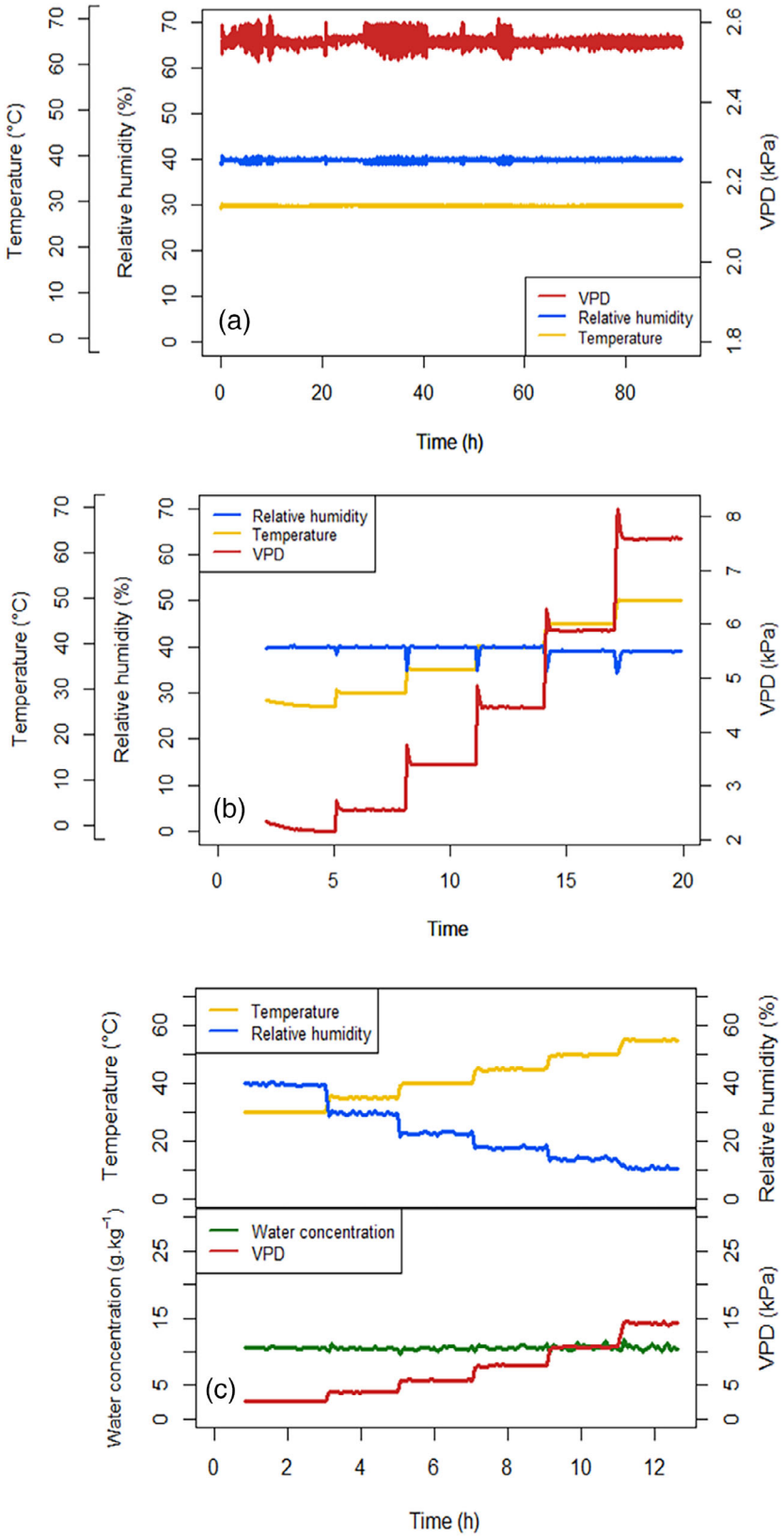

FIGURE 2 Time courses of environmental conditions inside the DroughtBox. (a) stable conditions, (b) ramps in temperature with stable relative humidity and (c) ramps in temperature with stable water vapor concentration

2.5 | Testing the temperature dependence of g_{res}

The aim of this experiment was to determine the phase transition temperature (T_p) by measuring g_{res} across a range of temperatures. For each species respectively, branches were exposed to a combination of increasing air temperature set at 30, 35, 40, 45, 50 and 55°C and decreasing RH set at 40, 30, 23, 18, 14 and 11% to maintain water concentration at 10.6 g kg^{-1}, except for *P. menziesii* which underwent an increase in temperature from 30 to 50°C with 5°C steps and a decrease in RH at 40, 30, 23, 18 and 14%. The duration (hours) of each temperature step varied as follows: 10, 3, 3, 3, 1 and 1 h for the conifer species and 6, 1, 1, 1, 0.75 and 0.75 h for *Q. ilex*, respectively. These sequences of time ensured that stomata had closed, that g_{res} was stable toward the end of each temperature step, and that branches did not run out of water at higher temperatures. At each temperature step, g_{res} was calculated using the driving force derived from leaf temperature measurements (see below). The temperature dependence of g_{res} was determined using an Arrhenius plot, which is the natural logarithm of g_{res} against the inverse of temperature in Kelvin.

2.6 | Air versus leaf temperature

We examined possible differences between air and leaf temperature for each of the five species evaluated in this study. Thus, four branches per species were sampled and installed inside the Drought-Box, as described above. A series of four thermocouples connected to a datalogger (CR1000, Campbell Scientific INC, Vincennes, France) was secured to a single leaf/needle of each of the four branches, while an additional two thermocouples were hung in the air. Branches were exposed to the same temperature and relative humidity conditions over the same time-period used to measure T_p, from 30 to 55°C, 40 to 11% RH during 10, 3, 3, 3, 1 and 1 h for the conifer species and 6, 1, 1, 1, 0.75 and 0.75 h for *Q. ilex*, respectively. Air and leaf temperature were logged every 15 s. These experiments were also conducted on oven-dried leaves in two species (*C. atlantica* and *Q. ilex*).

2.7 | Time to hydraulic failure

We assessed the time to hydraulic failure in a series of experiments using branches of two conifer species (*C. atlantica* and *P. abies*) dehydrated inside the Drought-Box under contrasting conditions. In experiment 1, eight branches of each species were dehydrated under constant and mild temperature (30°C) and RH (40%). In experiment 2, eight branches of each species were dehydrated under the same conditions as experiment 1, but were also exposed to a simulated heatwave, with temperature set to 46°C and RH set to 17%, for a period of 10 h, following maximum stomatal closure. During all experiments, the concentration of water in the air remained constant at ca. 10.6 g kg^{-1}. Branches were sampled and prepared for installation inside the Drought-Box as described above. Once installed, they were allowed to dehydrate over a period of up to 100 h in both experiments, during which time-individual branches were removed every 9–12 h. Upon removal, each branch was weighed (for fresh mass determination) and then sealed in a plastic bag for 10–15 min before being harvested for determination of water potential using a Scholander-type pressure chamber (PMS, PMS Instrument Company, Albany, USA) and percentage loss of conductance (PLC) at the branch level using X-ray microtomography (Micro-CT). All needles from each branch were collected and oven-dried for the determination of leaf dry mass, while the dry mass of the stem component of each branch was calculated from strong allometric relationships ($r^2 > 0.85$) between the leaf dry mass and the stem dry mass measured on 5–8 additional branches per species.

The PLC of each branch was determined by using Micro-CT, a technique that allows the evaluation of embolism formation and spreading by direct observation (Torres-ruiz, Cochard, Mencuccini, Delzon, & Badel, 2016, Dalla-Salda et al. 2014). Thus, each branch was adjusted to 60 mm length with a razor blade, immersed in wax to avoid dehydration during scanning and placed in an X-ray microtomograph (Nanotom 180 XS, GE, Wunstorf, Germany) at the PIAF laboratory (INRAE, Clermont-Ferrand, France). For the micro-CT image acquisition and image combination, the field of view was adjusted to $4.0 \times 4.0 \times 4.0$ mm^3 and the X-ray source set to 60 kV and 240 μA. For each ca. 21 min scan, 1,000 images were recorded during the 360° rotation of the sample. After 3D reconstruction, the

TABLE 1 g_{res} (mmol m^{-2} s^{-1}) ± standard errors for four conifers species (*Abies alba*, *Cedrus atlantica*, *Pseudotsuga menziesii* and *Picea abies*) and one angiosperm specie (*Quercus ilex*) the different temperature levels and T_p value (°C) for each specie

Species temperature (°C)	*A. alba* (mmol.m^{-2}.s^{-1})	*C. atlantica* (mmol.m^{-2}.s^{-1})	*P. menziesii* (mmol.m^{-2}.s^{-1})	*P. abies* (mmol.m^{-2}.s^{-1})	*Q. ilex* (mmol.m^{-2}.s^{-1})
30	0.76 ± 0.02	0.62 ± 0.10	0.90 ± 0.03	0.44 ± 0.03	1.64 ± 0.05
35	0.80 ± 0.03	0.68 ± 0.03	0.90 ± 0.02	0.48 ± 0.04	1.55 ± 0.07
40	0.82 ± 0.01	0.79 ± 0.02	0.97 ± 0.04	0.55 ± 0.03	1.63 ± 0.05
45	0.95 ± 0.02	1.11 ± 0.02	1.36 ± 0.02	0.66 ± 0.03	1.74 ± 0.07
50	1.22 ± 0.02	1.58 ± 0.05	1.90 ± 0.02	0.85 ± 0.02	1.92 ± 0.03
55	1.53 ± 0.02	2.78 ± 0.03	N. A.	1.00 ± 0.02	2.78 ± 0.06
TP (°C)	42.12	40.55	39.77	39.38	43.81

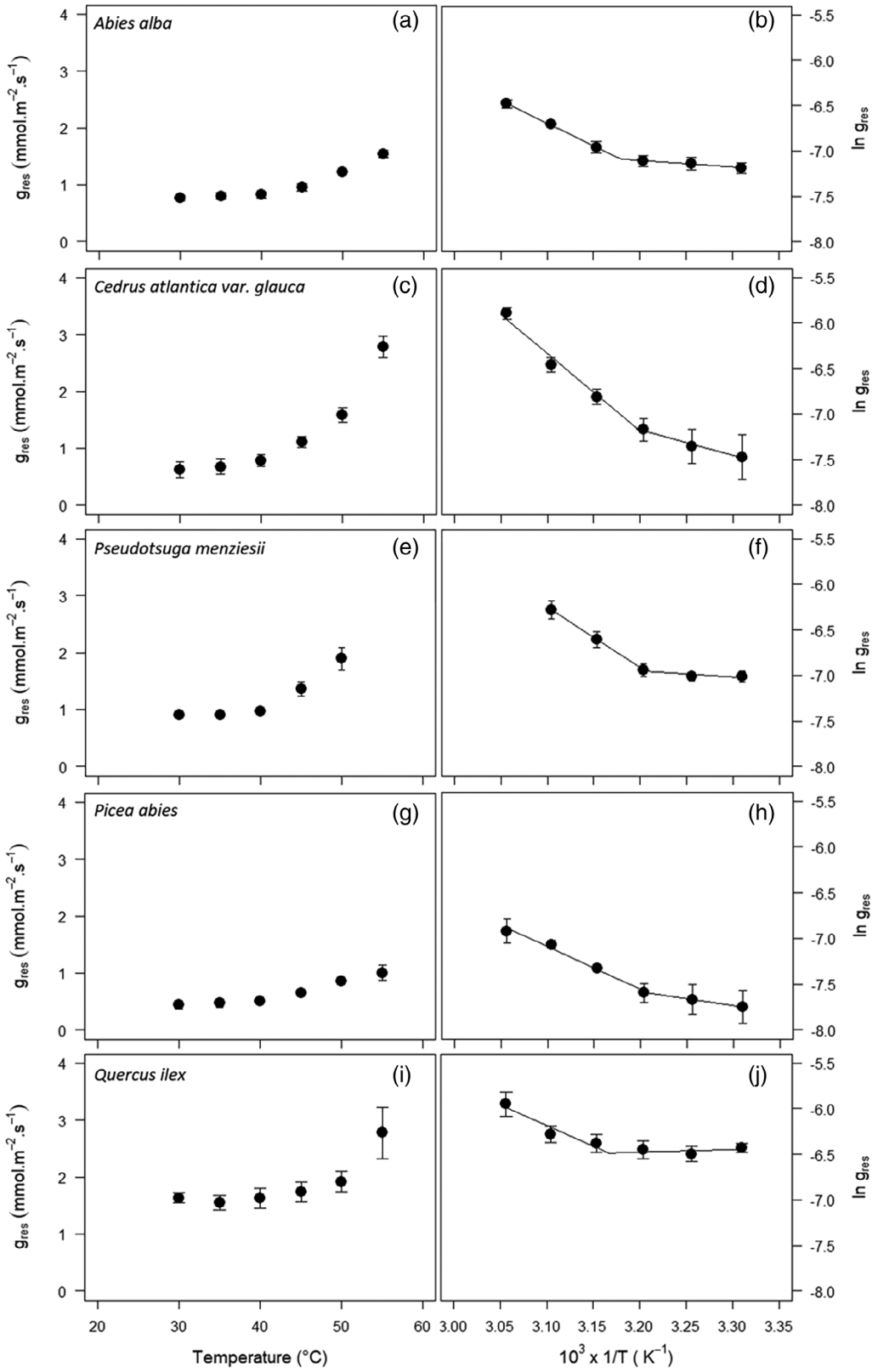

FIGURE 3 Plots showing the temperature dependence of g_{res} and the corresponding Arrhenius plot for *Abies alba* (a, b), *Cedrus atlantica* (c, d), *Pseudotsuga menziesii* (e, f), *Picea abies* (g, h) and *Quercus ilex* (i, j) from 30 to 55°C with stable water vapor concentration at 10.6 $g.kg^{-1}$

spatial resolution of the image was $2.00 \times 2.00 \times 2.00\ \mu m^3$ per voxel. One transverse 2D slice was extracted from the middle of the volume using VGStudio Max© software (Volume Graphics, Heidelberg, Germany). After scanning the sample, a second scan was performed after the sample was cut in the air just below the scanned area, inducing air entry in the remaining functional conduits and therefore 100% of embolized xylem in the area. PLC was then calculated by comparing the area occupied by embolized tracheids measured after the first scan and the total xylem conductivity area (A_e and A_c, respectively) as:

$$PLC = 100\frac{(A_e)}{(A_c)}$$

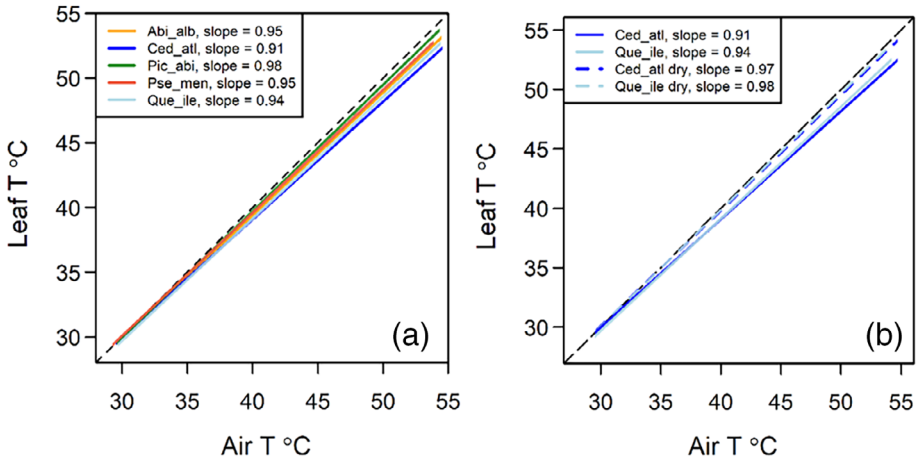

FIGURE 4 (a) The relationship between leaf and air temperature with increasing set temperature inside the Drought-Box across the four conifer (yellow = *Abies alba*; blue = Cedrus atlantica; green = *Picea abies*; red = *Pseudotsuga menziesii*) and one angiosperm (light blue = *Quercus ilex*) species. The slope of the leaf-air temperature relationship across set points is included for each species. (b) The relationship between leaf and air temperature (solid lines) and dry leaf and air temperature (dashed lines) with increasing set temperature inside the Drought-Box for the conifer Cedrus atlantica (blue) and the angiosperm *Quercus ilex* (light blue). The slope of the leaf-air temperature relationships across set points is included for each species

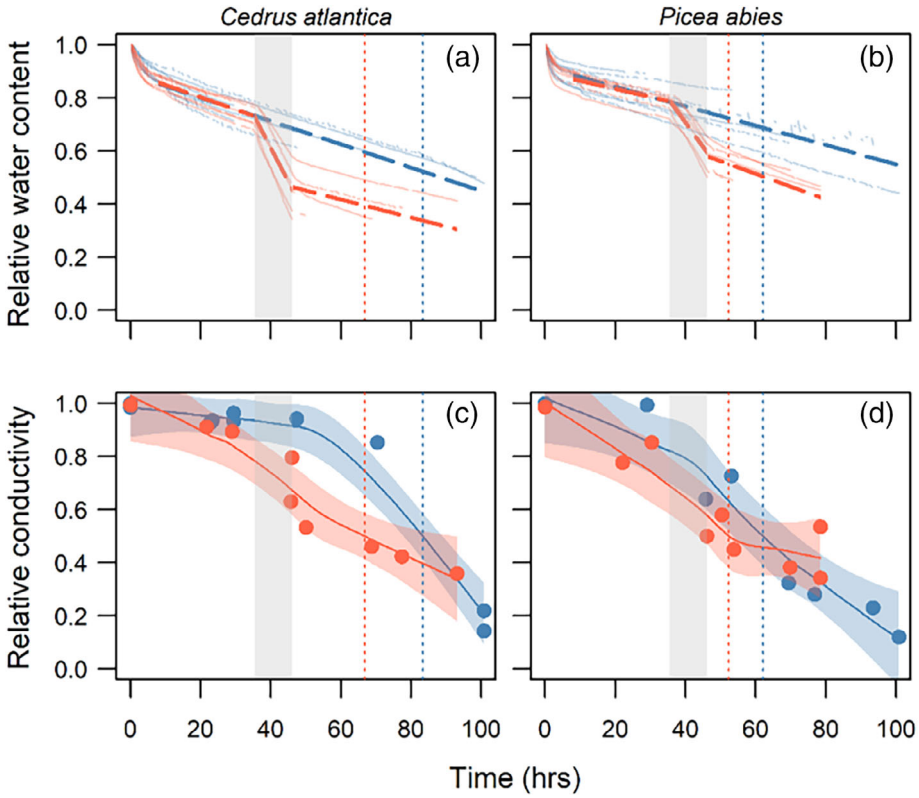

FIGURE 5 Plots showing changes in RWC (a–b) and percentage loss conductance (expressed as relative conductivity, c–d) for branches of two conifer species (Cedrus atlantica, [a, c]; and *Picea abies*, [b, d]) dehydrated under contrasting climate conditions inside the Drought-Box. Blue lines and symbols represent branches dehydrated under constant temperature (30°C) and relative humidity (40%); red lines and symbols represent branches dehydrated under constant temperature (30°C) and relative humidity (RH, 40%), but punctuated by a 10 h heatwave (grey shaded area) with temperature and RH set to 46°C and 17%, respectively

For each of Drought-Box experiments, the time to hydraulic failure was defined as the number of hours required for branches to dehydrate from full hydration to levels of water stress associated with 50% loss of theoretical conductivity, as determined from micro-CT measurements of PLC in branches during the experiments.

2.8 | Statistical analysis

Significant differences in g_{res} values were determined with ANOVA tests with $\alpha < 0.05$ followed by a Tukey HSD post-hoc or with a Kruskal Wallis test followed by Wilcoxon post hoc test when homoscedasticity of variances was not fulfilled. Spearman rank correlation test was used to test the effect of temperature increase on g_{res}. For the time to hydraulic failure experiments, the time (hours) at 50% loss of conductivity was determined using the *fitplc* function combined with a 'loess' model. The RWC at this time was determined from linear mixed-effects models fit to the branch relative water content (RWC) versus time data. The relationship between PLC and RWC over the course of dehydration was described using the *fitplc* function with a 'weibull' model.

3 | RESULTS

Set to a constant temperature of 30°C and a RH of 40%, both air T (30 ± 0.2°C) and RH (40 ± 1%) remained very stable during 90 hours of measurements (Figure 2a). When air temperature was increased in 5°C steps, from 25 to 50°C, and RH was held constant at 40%, RH maintained the target value (± 0.2%) following a brief decline as temperature increased (Figure 2b). At each step, temperature increased ~0.3°C above the target temperature, before stabilizing (± 0.01°C) after roughly 20 min. When water concentration was set to remain constant (at 10.6 $g.kg^{-1}$) across temperatures, RH took less than 10 min to reach the corresponding value (Figure 2c).

For each of the conifer species, the dynamics of plant water loss over time tended to follow three distinct phases represented by: A) a first short phase lasting a few hours with high rates of water loss until maximum stomata closure; B) a second phase characterized by a stable shallow slope, during which time stomata are closed but water loss continues via residual conductance (g_{res}); and C) a third phase characterized by a flattening of the slope as branch water content eventually reaches equilibrium with the ambient relative humidity (Figure S2). Branch residual conductance, measured at 30°C and at RH 40%,

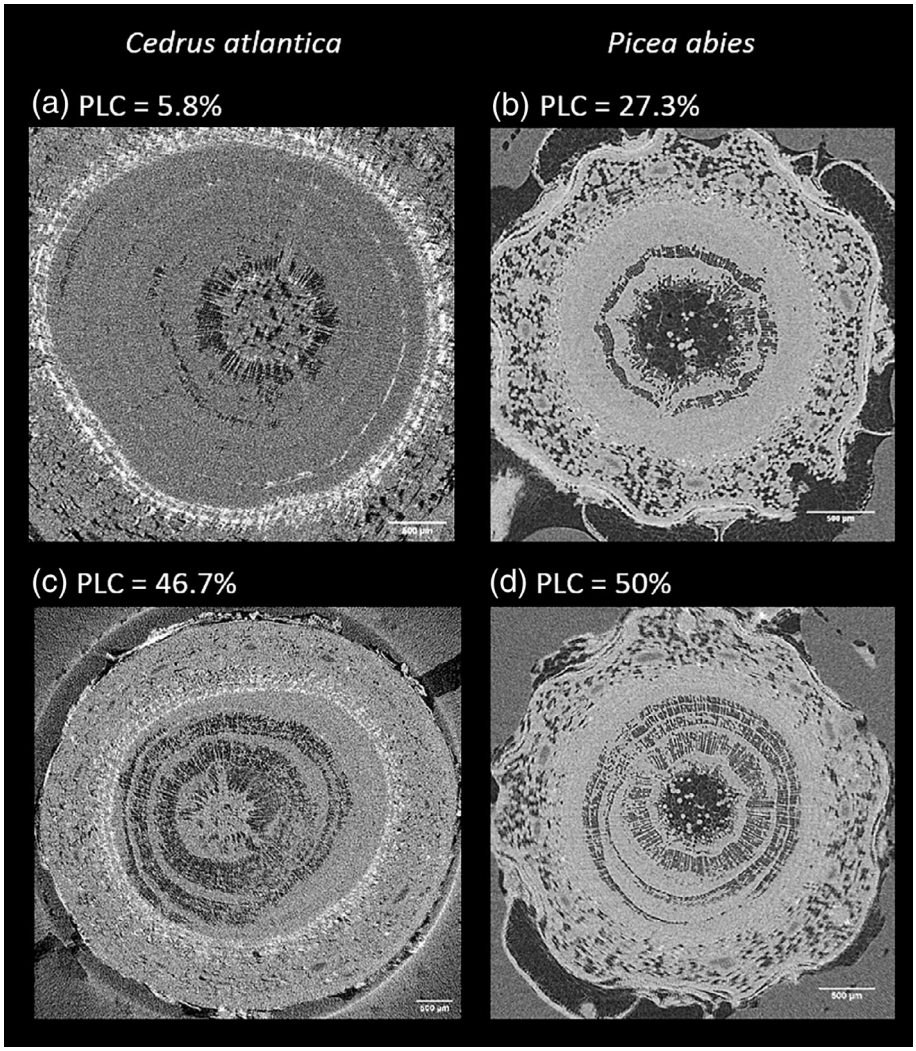

FIGURE 6 Transverse Micro tomography images of *Cedrus atlantica* (a and c) and *Picea abies* (b and d) obtained from control branches (a and b) and from branches that were exposed to heatwave (c and d). Conduits in grey and black represent those functional or cavitated tracheids, respectively. PLC indicates the theoretical loss of hydraulic conductivity for each image. Scale bars = 500 μm

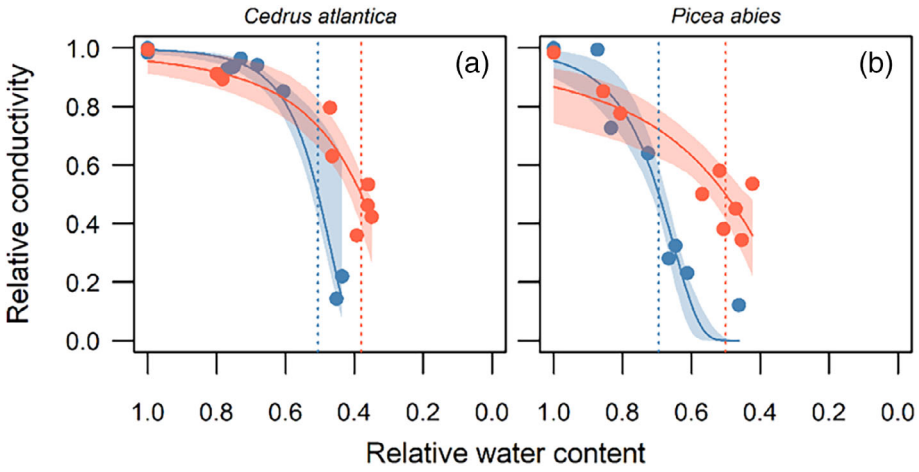

FIGURE 7 The relationship between relative conductivity of stem xylem (PLC) and RWCof branches of *Cedrus atlantica* (a) and *Picea abies* (b) dehydrated inside the Drought-Box under constant temperature and relative humidity (blue lines and symbols) and under the same conditions but punctuated by a heatwave event (red lines and symbols). Dashed vertical lines represent the RWC at 50% loss in conductivity. Note that for both species, PLC is decoupled from RWC under heatwave conditions

varied among the four conifers, ranging from 0.44 mmol m^{-2} s^{-1} in *P. abies* to 0.9 mmol m^{-2} s^{-1} in *Pseudotsuga menziesii*, while for the angiosperm *Q. ilex*, g_{res} was 1.64 mmol m^{-2} s^{-1} (Table 1). Measured across a range of temperatures, from 30–55°C, all species showed a similar bi-phasic response whereby g_{res} increased significantly with increasing temperature > 39°C (Figure 3). Among the four conifer species, T_p values were similar, ranging from 39.4°C in *P. abies* to 42.1°C in *A. alba*, while the highest T_p value was 43.8°C recorded for *Q. ilex* (Table 1, Figure 3).

In all five species, leaf temperature tended to be lower than air temperature during dehydration (following stomatal closure), with air-leaf temperature differences increasing with increasing set temperature (Figure 4). At 30°C, air-leaf temperature differences were relatively small across species, ranging from 0.02°C for *Pseudotsuga menziesii* to 0.3°C for *Q. ilex*, while at 55°C, air-leaf temperature differences were larger, ranging from 0.76°C for *P. abies* to 2.51°C for *C. atlantica* (Figure 4a). In contrast, when using oven-dried leaves of *C. atlantica* and *Q. ilex*, leaf-air temperature differences were smaller across all temperature set points, with a maximum difference of 0.71°C recorded for *C. atlantica* at 55°C (Figure 4b). The accumulated difference between leaf and air temperature across the temperature set points was unrelated to g_{min} recorded either at 30°C or at 50°C across species (Figure S3).

Under constant temperature and relative humidity, the recorded time to hydraulic failure was shorter in *P. abies* (62.1 hrs) compared to *C. atlantica* (83.3 h). The heatwave treatment increased the occurrence of xylem cavitation (see Figure 6) and resulted in a reduction in the time to hydraulic failure of 9.7 hrs in *P. abies* and 16.5 hrs in *C. atlantica* (Figure 5c,d). The corresponding RWC at this point in time was 0.51 and 0.69, under constant conditions, and 0.38 and 0.50, under constant × heatwave conditions for *C. atlantica* and *P. abies*, respectively (Figure 5a,b). In response to the heatwave event, the relationship between PLC and RWC became decoupled, with 50% loss of conductivity occurring at much lower RWC values in both species when dehydrated under constant × heatwave conditions compared to constant conditions (Figure 7).

4 | DISCUSSION

There is increasing awareness of residual water loss from leaves and stems (g_{res}) as a key determinant of the timing of hydraulic failure and tree mortality during drought (Blackman et al., 2016; Martin-StPaul et al., 2017). Furthermore, knowledge of the response of g_{res} to increasing temperature will further increase our understanding of tree mortality risk during hot-drought events (Cochard, 2019). As a result, an increasing demand for measurements of g_{res} and the transition-phase temperature (T_p) across diverse species can be expected in the near future. However, a reference tool and a standard protocol for determining these parameters have been lacking. The DroughtBox is intended to meet this need by allowing users to measure g_{res} under stable and variable air T and RH conditions, as well as to assess species time to hydraulic failure during simulated drought and/or drought by heatwave events.

A fine control of air temperature and relative humidity and keeping both variables stable is essential for evaluating residual water loss from leaves and branches accurately. Until now, this condition has been difficult to attain, especially when using the standard bench dehydration method (Scoffoni and Sack, Minimum epidermal conductance, PrometheusWiki), being necessary the use of incubators able to control air temperature but not relative humidity automatically (e.g., Schuster et al., 2016). Our test measurements show that the DroughtBox is able to maintain very stable conditions of temperature and relative humidity across a range of set points needed for measuring both g_{res} and T_p (Figure 2). With the added element of automated measurements of changes in branch mass, the DroughtBox represents a significant improvement for evaluating these parameters across species.

In the current study, g_{res} (measured at 30°C and at 40% RH) varied among species, ranging from 0.4 mmol m^{-2} s^{-1} in the conifer *P. abies* to 1.64 mmol m^{-2} s^{-1} in the angiosperm *Q. ilex*. These values are broadly consistent with previous measurements of g_{min} in these species groups (Duursma et al., 2019). This suggests that g_{res}, representing the combined residual conductance from leaves and stems (i.e., the bark or lenticular conductance), is broadly comparable with

previous measurements made solely on leaves. Although we did not measure bark conductance separately we believe that the bark component likely played a small role in our measurements of g_{res} considering that the surface area of the stem was relatively low (<5% across species) compared to that of the leaves. Additionally, while measuring g_{min} in the DroughtBox would be challenging for small conifer needles, we have successfully measured g_{min} in two angiosperm species with larger leaves (data not shown).

A major advantage of the DroughtBox is that it can be programmed to assess the temperature dependence of g_{res} (Burghardt & Riederer, 2006). This is important because temperature is known to have a significant effect on cuticular transpiration (Burghardt & Riederer, 2006), especially beyond the transition phase temperature T_p, which exposes plants to greater risk of mortality (Cochard, 2019). In the current study, we observed T_p values for small branches ranging from 39.4°C in *P. abies* to 43.8°C in *Q. ilex*. These values are consistent with the few previous measurements of T_p in temperate and arid-zone species (Bueno et al., 2019; Burghardt & Riederer, 2006; Schuster et al., 2016). They also broadly fit with each species climatic niche, with *P. abies* occurring in cool-wet regions of northern Europe and *Q. ilex* occurring in warm-arid regions of the Mediterranean, suggesting that T_p may be under selective pressure as an important driver of plant fitness during drought across climates. This is consistent with previous studies that have highlighted the importance of high T_p in drought resistant desert plants (Bueno et al., 2019; Schuster et al., 2016). In fact, evidence to date suggests that, compared to temperate species, hot desert plants may have a different cuticle composition that confer greater thermostability and thus a more stable g_{res} even under high temperatures (Bueno et al., 2019). However, there is a need to increase the number of T_p values measured across diverse species before the links with climate and ecological strategy and also with cuticle composition can be tested robustly.

The DroughtBox is also ideal for making measurements of the time for branches to dehydrate to critical levels of hydraulic failure (50% loss of xylem conductivity) under stable and/or variable climatic conditions. In our study, a longer time to hydraulic failure was recorded in *C. atlantica* than in *Picea abies* under fixed 30°C conditions, even though g_{res} was found to be higher in *C. atlantica* (Table 1). This suggests other traits such as cavitation resistance, which is known to be higher in *C. atlantica* than in *Picea abies* (Choat et al., 2012), should be taken into account when determining time to hydraulic failure. For both species, the simulated heatwave event resulted in a strong reduction in time to hydraulic failure, confirming that plants are at higher risk of mortality when facing hot-drought events (Cochard, 2019). While the 46°C heatwave exceeded T_p values of both species, a greater reduction in the time to hydraulic failure was recorded in *C. atlantica*. This response may be due to the greater temperature sensitivity of g_{res} recorded in this species (see Figure 3), the mechanism of which is likely related to specific temperature response characteristics of the leaf cuticle (Bueno et al., 2019; Schuster et al., 2016). Additionally, the heatwave acted to decouple the relationship between PLC and branch RWC during drought, with greater relative water loss at a common level of PLC (50%) in branches when exposed to the heatwave. This suggests that there may be a significant contribution of water loss from leaves and or branches in response to heatwave events and furthermore implies that branch RWC is not a reliable predictor of hydraulic failure in plants exposed to hot-drought conditions.

In conclusion, the DroughtBox is a novel tool that allows for accurate measurements of both g_{res} and T_p under controlled conditions. Residual water loss from plants is increasingly studied due to its strong impact on the time to hydraulic failure during drought and, therefore, its relevance when evaluating the risk of drought-induced tree mortality. An increased knowledge of species T_p will enable researchers to model species responses during heat and drought events associated with a warming climate and also to get better projections of the risk of forest dieback and changes in tree species distribution. The DroughtBox improves upon previous techniques for measuring g_{res} that are either laborious, with repeated measurements of leaf mass on a balance, or lacked climate control of VPD. By being fully programmable, the DroughtBox not only allows physiological traits related with the thermostability of g_{res}, such as T_p, to be phenotyped, but also the dynamics of branch dehydration and time to hydraulic failure under a range of simulated climate conditions.

ACKNOWLEDGMENTS

The authors thank Pierre Conchon for his technical assistance with Micro-CT and the Office National des Forêt and the Arboretum of Royat for allowing them to sample branches. This research was funded by the project ANR-18-CE20-0005 *Hydrauleaks*.

CONFLICT OF INTEREST

None declared.

AUTHOR CONTRIBUTION

HC and JMTR: conceived and design of the DroughtBox. JC and RS constructed the first prototype, developed the programs for running it and provided substantial technical support during the measurements. LMB and CJB were responsible of running the measurements and carried out the data analysis. LMB, CJB, HC and JMTR interpreted the results. LMB and CJB wrote the manuscript with input from HC, JMTR and AH.

ORCID

Eric Badel https://orcid.org/0000-0003-2282-7554

REFERENCES

Allen, C. D., Macalady, A. K., Chenchouni, H., Bachelet, D., McDowell, N., Vennetier, M., … Cobb, N. (2010). A global overview of drought and heat-induced tree mortality reveals emerging climate change risks for forests. *Forest Ecology and Management*, *259*, 660–684.

Arve, L., Torres, S., Olsen, J. E., & Tanino, K. K. (2011). Stomatal responses to drought stress and air humidity. In A. Shanker (Ed.), *IntechAbiotic Stress in Plants - Mechanisms and Adaptations* (pp. 267–280). Rijeka, Croatia: INTECH.

Blackman, C. J., Brodribb, T. J., & Jordan, G. J. (2012). Leaf hydraulic vulnerability influences species' bioclimatic limits in a diverse group of woody angiosperms. *Oecologia*, *168*, 1–10.

Blackman, C. J., Creek, D., Maier, C., Aspinwall, M. J., Drake, J. E., Pfautsch, S., … Meinzer, F. (2019). Drought response strategies and hydraulic traits contribute to mechanistic understanding of plant dry-down to hydraulic failure. *Tree Physiology*, *39*, 910–924.

Blackman, C. J., Pfautsch, S., Choat, B., Delzon, S., Gleason, S. M., & Duursma, R. A. (2016). Toward an index of desiccation time to tree mortality under drought. *Plant Cell and Environment*, *39*, 2342–2345.

Brodribb, T., & Hill, R. S. (1999). The importance of xylem constraints in the distribution of conifer species. *New Phytologist*, *143*, 365–372.

Brodribb, T. J., McAdam, S. A. M., Jordan, G. J., & Martins, S. C. V. (2014). Conifer species adapt to low-rainfall climates by following one of two divergent pathways. *Proceedings of the National Academy of Sciences*, *111*, 14489–14493.

Bueno, A., Alfarhan, A., Arand, K., Burghardt, M., Deininger, A.-C., Hedrich, R., … Riederer, M. (2019). Temperature effects on the cuticular transpiration barrier of two desert plants with water-spender and water-saver life strategies. *Journal of Experimental Botany*, *70*, 1613–1625.

Burghardt, M., & Riederer, M. (2003). Ecophysiological relevance of cuticular transpiration of deciduous and evergreen plants in relation to stomatal closure and leaf water potential. *Journal of Experimental Botany*, *54*, 1941–1949.

Burghardt, M., & Riederer, M. (2006). Cuticular transpiration. In M. Riederer & C. Müller (Eds.), *Biology of the plant cuticle* (pp. 292–311). Oxford: Blackwell Publishing.

Chapotin, S. M., Razanameharizaka, J. H., & Holbrook, N. M. (2006). Baobab trees (Adansonia) in Madagascar use stored water to flush new leaves but not to support stomatal opening before the rainy season. *New Phytologist*, *169*, 549–559.

Choat, B., Jansen, S., Brodribb, T. J., Cochard, H., Delzon, S., Bhaskar, R., … Zanne, A. E. (2012). Global convergence in the vulnerability of forests to drought. *Nature*, *491*, 752–755.

Cochard, H. (2019). A new mechanism for tree mortality due to drought and heatwaves. *bioRxiv* 531632. https://doi.org/10.1101/531632.

Creek, D., Lamarque, L. J., Torres-ruiz, J. M., Parise, C., Burlett, R., & David, T. (2020). Xylem embolism in leaves does not occur with open stomata: Evidence from direct observations using the optical visualization technique. *Journal of Biological Chemistry*, *71*, 1151–1159.

Dalla-Salda, G., Fernández, M. E., Sergent, A.-S., Rozenberg, P., Badel, E., & Martinez-Meier, A. (2014). Dynamics of cavitation in a Douglas-fir tree-ring: transition-wood, the lord of the ring?. *Journal of Plant Hydraulics*, *1*, e005. https://doi.org/10.20870/jph.2014.e005

Darwin, F.1898. Observations on stomata. *Philosophical Transactions of the Royal Society of London Series B190*: 531–621.

Duursma, R. A., Blackman, C. J., Lopéz, R., Martin-StPaul, N. K., Cochard, H., & Medlyn, B. E. (2019). On the minimum leaf conductance: Its role in models of plant water use, and ecological and environmental controls. *New Phytologist*, *221*, 693–705.

Gleason, S. M., Blackman, C. J., Cook, A. M., Laws, C. A., & Westoby, M. (2014). Whole-plant capacitance, embolism resistance and slow transpiration rates all contribute to longer desiccation times in woody angiosperms from arid and wet habitats. *Tree Physiology*, *34*, 275–284.

Jentsch, A., Kreyling, J., & Beierkuhnlein, C. (2007). A new generation of climate-change experiments: Events, not trends. *Frontiers in Ecology and the Environment*, *5*, 365–374.

Martin-StPaul, N., Delzon, S., & Cochard, H. (2017). Plant resistance to drought depends on timely stomatal closure. *Ecology Letters*, *20*, 1437–1447.

Schuster, A. C., Burghardt, M., Alfarhan, A., Bueno, A., Hedrich, R., Leide, J., … Riederer, M. (2016). Effectiveness of cuticular transpiration barriers in a desert plant at controlling water loss at high temperatures. *AoB Plants*, *8*.

Schuster, A. C., Burghardt, M., & Riederer, M. (2017). The ecophysiology of leaf cuticular transpiration: Are cuticular water permeabilities adapted to ecological conditions? *Journal of Experimental Botany*, *68*, 5271–5279.

Sperry, J. S., Alder, N. N., & Eastlack, S. E. (1993). The effect of reduced hydraulic conductance on stomatal conductance and xylem cavitation. *Journal of Experimental Botany*, *44*, 1075–1082.

Torres-ruiz, J. M., Cochard, H., Mencuccini, M., Delzon, S., & Badel, E. (2016). Direct observation and modelling of embolism spread between xylem conduits: A case study in Scots pine. *Plant, Cell & Environment*, *39*, 2774–2785.

Tyree, M. T. (1989). Vulnerability of xylem to cavitation and embolism. *Annual Review of Plant Physiology and Plant Molecular Biology*, *40*, 19–38.

Tyree, M. T., & Ewers, F. W. (1991). The hydraulic architecture of trees and other woody plants. *New Phytologist*, *119*, 345–360.

SUPPORTING INFORMATION

Additional supporting information may be found online in the Supporting Information section at the end of this article.

How to cite this article: Billon LM, Blackman CJ, Cochard H, et al. The DroughtBox: A new tool for phenotyping residual branch conductance and its temperature dependence during drought. *Plant Cell Environ*. 2020;1–11. https://doi.org/10.1111/pce.13750